

Research Article

Abl Activation Reduces Parkin Activity and Arrests Autophagy

Lonskaya I¹, Hebron M¹, Chen W^{1,2}, Feng Y¹, Schachter JB³ and Moussa C^{1*}

¹Department of Neurology, Laboratory for Dementia and Parkinsonism, Georgetown University Medical Center, USA

²Department of Traditional Chinese Medicine, Xuanwu Hospital, Capital Medical University, China

³Neuroscience Discovery, Merck Research Laboratories, USA

*Corresponding author: Charbel E Moussa, Department of Neurology, Laboratory for Dementia and Parkinsonism, Georgetown University School of Medicine, USA

Received: August 09, 2016; Accepted: October 26, 2016; Published: October 31, 2016

Abstract

The non-receptor tyrosine kinase Abelson (Abl) is activated in neurodegeneration and regulates Parkin activity *via* unknown mechanisms. Parkin plays a critical role in autophagic clearance of toxic protein accumulation. To study the effects of Abl activation on Parkin, lentiviral Tau or A β 42 were expressed in the hippocampus of 1-year old Tet-off mice that conditionally express active Abl (AbIPP/tTA). Abl activation reduces endogenous Parkin activity and arrests autophagic flux in brains accumulating Tau and A β 42. Our analysis suggests that Abl activation regulates Parkin activity via ubiquitination. Abl activation also decreases Parkin stability, leading to accumulation of insoluble protein. Since Parkin expression promotes autophagic clearance of p-Tau and A β 42 and protects against cell death, these new data suggest that Abl inhibition is an alternative strategy to activate Parkin and reduce protein accumulation in neurodegenerative diseases.

Keywords: Abl; Parkin; Autophagy; Tau; A β 42

Introduction

Abelson (Abl) encodes a protein tyrosine kinase that is distributed in the nucleus and the cytoplasm and is involved in a wide range of functions [1]. Abl activation is implicated in a number of neurodegenerative diseases [2-5]. Phosphorylated Abl is detected with both neuritic plaques and Neuro Fibrillary Tangles (NFTs) in the hippocampus and entorhinal cortex in Alzheimer's Disease (AD) [3,5-7]. In AD mouse models β -amyloid (A β) activates Abl and Tau hyper-phosphorylation (p-Tau), while Abl inhibition reduces A β and p-Tau and reverses cognitive decline [8,9]. Intracranial injection of A β fibrils into the mouse hippocampus up-regulates Abl [9]. In primary neuronal culture, Abl inhibition prevents A β fibrillation and cell death [10].

Some studies suggest that Abl activation directly phosphorylates Parkin to alter Parkin's E3 ubiquitin ligase function [2,4,11], thereby altering Parkin regulation of autophagy and proteasome activity [12-15]. Mutations in the gene coding for Parkin (Park2) are associated with autosomal recessive early onset Parkinson Disease (PD) [16]. Parkin stability is reduced in the nigrostriatum of sporadic PD [4,17] and temporal lobe of AD brains [17-19]. Relevant to AD pathology, A β accumulation leads to formation of undigested autophagic vacuoles. Parkin expression enhances autophagic clearance of A β and resolves undigested autophagic vacuole accumulation [18,20,21]. Pharmacologic inhibition of Abl increases Parkin activity and reduces A β and p-Tau in models of neurodegeneration [22-25].

In the current studies we evaluated the role of Abl activation on Parkin modification, including phosphorylation, ubiquitination and activity. We used lentiviral delivery of either human four repeat (4R) Tau or A β 42 into the hippocampus of 1-year old conditional mice (AbIPP/tTA) that express active Abl under a neuron-specific promoter (CamKII α) regulated by doxycycline (Tet-off) [26]. We determined the effects of Abl activation on Parkin modification and

autophagic p-Tau and A β 42 clearance after 6 weeks of Abl activation via Doxycycline (Dox) withdrawal. The results indicate that Abl activation reduces Parkin ubiquitination, and thereby reduces Parkin activity. This leads to a decrease in Parkin solubility that is reminiscent of Parkin modification in PD and AD.

Materials and Methods

Stereotaxic injection

We used lentiviral gene delivery of 4R human Tau or A β 42 into the CA1 hippocampus of 1 year old AbIPP/tTA mice [26]. Peter Davies's group generated conditional mice under a neuron-specific promoter (CamKII α) regulated by Dox (Tet-off) to express active Abl [26]. AbIPP/tTA mouse colony is viable and expresses active T412 Abl when taken off-dox for 6 weeks. Stereotaxic surgery was performed on AbIPP/tTA mice to inject 1x10⁹ m.o.i (Multiplicity of Infection) lentiviral Tau or A β 42 with and without 1x10⁹ m.o.i lentiviral Parkin or LacZ into hippocampus as previously described [21,27-29]. Males and females were divided into group 1 on-Dox and group 2 off-Dox (control chow) for 3 weeks and stereotaxic surgery was performed, leading to gene expression in the entire mouse hemisphere [21]. Mice were sacrificed 3 weeks post-injection (total period of Dox withdrawal was 6 weeks). All experiments were conducted in full compliance with the recommendations of Georgetown University Animal Care and Use Committee (GUAUC).

Cell Culture and transfection

Human neuroblastoma M17 cells were grown in 24 well dishes (Falcon) and transiently transfected with 3 μ g human wild type or mutant T240R Parkin cDNA for 24 hours. Cells were then either transfected with 3 μ g Abl shRNA for 24hr or treated with 10Mm Nilotinib (AMN-107, Shellacked Chemical, LLC, USA) or DMSO (1 μ L) for 24 hours and harvested after a total of 48 hours of transfection for Western blot and immunoprecipitation.

Western blot (WB) analysis

The brain was isolated and tissues will be homogenized in 1x STEN buffer (50 mM Tris (pH 7.6), 150 mM NaCl, 2 mM EDTA, 0.2 % NP-40, 0.2 % BSA, 20 mM PMSF and protease cocktail inhibitor), centrifuged at 10,000 x g for 20 min at 4°C and the supernatant containing the soluble protein fraction was collected. To extract insoluble A β 42, the pellet was re-suspended in 30% formic acid and centrifuged at 10,000 g for 20 min at 4°C and the supernatant was collected. Extracts were analyzed by Western Blot (WB) on SDS NuPAGE 4-12% Bis-Tris gel (Invitrogen, NP0301BOX). β -actin was probed (1:1000) with polyclonal antibody (ThermoScientific, PA121167). Total Abl was probed with (1:500) rabbit polyclonal antibody (Thermo Fisher) and p-Abl (Y214) with (1:500) rabbit polyclonal antibody (Millipore). Total Parkin was probed and immunoprobed (1:1000) with PRK8 antibody (Pierce), and Parkin phospho-serine65 was probed (1:500) with Rabbit polyclonal antibodies (Abcam). A rabbit polyclonal (Pierce) anti-LC3 (1:1000) antibody and lysosomal fractions were probed with (1:1000) rabbit polyclonal Lysosomal associated membrane protein-2 (LAMP2) antibodies (Abcam) were used. Rabbit anti-ubiquitin (Santa Cruz Biotechnology) antibody (1:1000) and total phospho-tyrosine antibody (1:2000) 4G10 (EMD Millipore) were used. Total tau was probed (1:1000) with Tau-5 monoclonal antibody (Chemicon, Temecula, CA, USA), and phosphorylated tau was probed (1:1000) with epitopes against polyclonal serine-396 (Chemicon, Temecula, CA, USA), polyclonal AT8 (1:1000) Serine-199/202 (Biosource, Carlsbad, CA, USA), polyclonal AT180 (1:1000) threonine-231 (Biosource, Carlsbad, CA, USA) and monoclonal (1:1000) human specific (HT7) antibody (Thermo Scientific). WBs were quantified by densitometry using Quantity One 4.6.3 software (Bio Rad).

Immunoprecipitation

Mouse brains were homogenized in 1XSTEN buffer and the soluble fraction was isolated as indicated above. The lysates were pre-cleaned with immobilized recombinant protein G agarose (Pierce #20365), and centrifuged at 2500 x g for 3 min at 4°C. The supernatant was recovered and quantified by protein assay and a total of 100 mg protein was incubated for 1 h at 4°C with primary 1:100 mouse anti-Parkin (PRK8) antibodies in the presence of sepharose G and an IgG control with primary antibodies. The immunoprecipitates were collected by centrifugation at 2500 x g for 3 min at 4°C, washed 5x in PBS, with spins of 3 min, 2500 x g using detergent-free buffer for the last washing step and the proteins were eluted according to Pierce instructions (Pierce #20365). After IP, the samples were size-fractionated on 4–12% SDS-NuPAGE and transferred onto 20 μ m nitrocellulose membranes.

Immuno histo chemistry (IHC) of brain sections

Animals were deeply anesthetized with a mixture of Xylazine and Ketamine (1:8), washed with 1X saline for 1 min and then perfused with 4% Para Formaldehyde (PFA) for 15-20 min. Brains were quickly dissected out and immediately stored in 4% PFA for 24h at 4°C, and then transferred to 30% sucrose at 4°C for 48h. Tissues were cut using a cryostat at 4°C into 20 μ m thick sections and stored at -200C. Mouse monoclonal (6E10) antibody (1:100) with DAB were used (Covance) followed by DAB staining. Tau staining was performed with HT7 (1:1000), AT180 (1:5000) and AT8 (1:3000) followed by DAB staining according to manufacturer's instructions

(Sigma). Cupric silver staining that detects degenerating fibers and neurons was also performed according to manufacturer's protocol (FD Neurotechnologies, Baltimore,MD). Stereological methods were applied by a blinded investigator using unbiased stereology analysis (Stereologer, Systems Planning and Analysis, Chester, MD) as previously described [21,27-29].

Subcellular fractionation for isolation of autophagic compartments

To determine autophagic flux in vivo, 0.5g of animal brains were homogenized at low speed (Cole-Palmer homogenizer, LabGen 7, 115 Vac) in 1xSTEN buffer and centrifuged at 1,000g for 10 minutes to isolate the supernatant from the pellet. The pellet was re-suspended in 1xSTEN buffer and centrifuged once to increase the recovery of lysosomes. The pooled supernatants were centrifuged at 100,000 rpm for 1h at 4°C to extract the pellet containing Autophagic Vacuoles (AVs) and lysosomes. The pellet was re-suspended in 10 ml (0.33 g/ml) 50% Metrizamide and 10 ml in cellulose nitrate tubes. A discontinuous Metrizamide gradient was constructed in layers from bottom to top as follows: 6 ml of pellet suspension, 10 ml of 26%; 5 ml of 24%; 5 ml of 20%; and 5 ml of 10% Metrizamide [30]. After centrifugation at 10,000 rpm for 1 hour at 4°C, the fraction floating on the 10% layer (Lysosome) and the fractions banding at the 24%/20% (AV 20) and the 20%/10% (AV10) Metrizamide inter-phases were collected by a syringe and examined via p-Tau and A β 1-42 specific ELISA.

A β 42 and p-Tau and α -synuclein enzyme-linked immunosorbent assay (ELISA)

Specific p-Tau ser396 (Invitrogen, KHB7031), AT8 (Invitrogen, KHB7041), AT180 (Invitrogen, KHB7031), human A A β 42 (Invitrogen, KHB3442,) and α -Synuclein (Invitrogen, KHB0061) ELISA were performed according to manufacturer's protocol. Caspase-3 activity assays were performed according to manufacturer's protocol as we previously described [21,27-29].

Transmission electron microscope (EM)

Brain tissues were fixed in (1:4, v:v) 4% PFA-picric acid solution and 25% glutaraldehyde overnight, then washed 3x in 0.1 M cacodylate buffer and osmicated in 1% osmium tetroxide/1.5% potassium ferrocyanide for 3h, followed by another 3x wash in distilled water. Samples were treated with 1% uranyl acetate in maleate buffer for 1 h, washed 3x in maleate buffer (pH 5.2), then exposed to a graded cold ethanol series up to 100% and ending with a propylene oxide treatment. Samples were embedded in pure plastic and incubated at 60°C for 1–2 days. Blocks were sectioned on a Leica ultracut microtome at 95 nm, picked up onto 100 nm formvar-coated copper grids and analyzed using a Philips Technai Spirit transmission EM.

Statistical analysis

All statistical analysis was performed using a GraphPad Prism, version 5.0 (GraphPad software, Inc, San Diego, CA). The number (N) indicates the number of independent experiments (cell culture) or number of individual animals. Asterisks designate significantly different as indicated, all data are presented with Mean \pm SEM, with actual p-values obtained using ANOVA with Neumann Keuls multiple comparison.

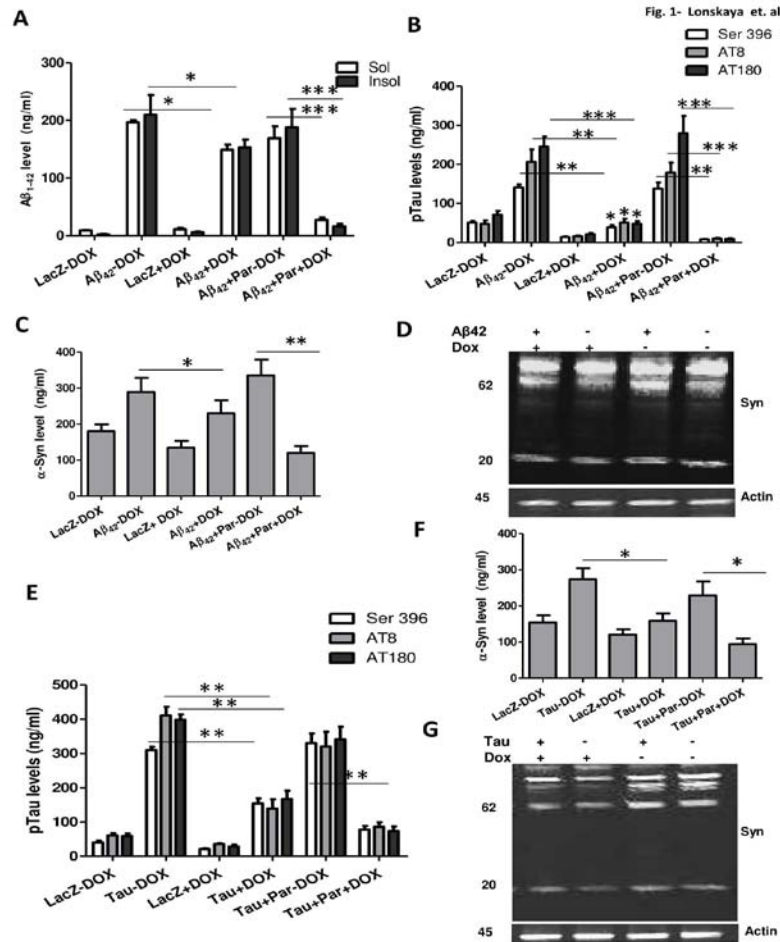


Figure 1: Abl activation increases Aβ₄₂, α-Synuclein and p-Tau levels. Concentration of human (A). Aβ₄₂ (B). mouse p-Tau (C). α-Synuclein in total brain lysates from AblPP/tTA mice expressing lentiviral Aβ₄₂ with and without Parkin±Dox (D). Western blot analysis on 4-12% NuPAGE gel showing α-Synuclein and actin (E). mouse p-Tau (F). α-Synuclein in total brain lysates from AblPP/tTA mice expressing lentiviral Tau with and without Parkin±Dox and (G). Western blot analysis on 4-12% NuPAGE gel showing α-Synuclein and actin. Graphs are mean±SEM, ANOVA with Neumann Keuls multiple comparison. N=4, asterisks are statistically significant compare to same treatment ±Dox or as indicated on graph. *indicates p<0.05, **P<0.01, ***P<0.001.

Parkin activity and solubility

To evaluate Abl effects on endogenous Parkin we determined Parkin solubility via fractionation of soluble (supernatant) and insoluble (pellet re-suspended in 4M urea) Parkin and performed WB with anti-total Parkin (PRK8) antibodies. To determine whether Parkin level correlates with its enzymatic activity, we immunoprecipitated Parkin (1:100) with anti-Parkin antibody (PRK8) from mouse brain lysates and measured its E3 ubiquitin ligase activity using E3LITE customizable ubiquitin ligase kit (LifeSensors, Cat# UC101). E3LITE measures the mechanisms of E1-E2-E3 activity in the presence of different ubiquitin chains as we previously described [21,27-29]. Ubch7 as an E2 that provides maximum activity with Parkin E3 ligase and add E1 and E2 in the presence of recombinant ubiquitin, K0 or K48 or K63 to determine the lysine-linked type of ubiquitin. E3 was added to an ELISA microplate that captures polyubiquitin chains formed in the E3-dependent reaction, which is initiated with ATP at RT for 60 minutes and read on a chemiluminescence plate reader.

Results

Abl activation increases Aβ₄₂, α-synuclein and p-tau levels

Lentiviral expression of human Aβ₄₂ in AblPP/tTA mice brains results in a significant increase in soluble and insoluble Aβ₄₂ (Figure 1A, N=4, p<0.05) with -Dox (Abl induced) compared to +Dox (Abl not induced). Co-expression of human Parkin with Aβ₄₂ significantly reduced Aβ₄₂ with +Dox, but induction of Abl expression by Dox withdrawal abrogated Parkin’s effects on Aβ₄₂ (Figure 1A, N=4, p<0.01). No Aβ₄₂ was detected in LacZ injected mice (indicated as -Aβ₄₂ in figures). The concentration of p-Tau epitopes, including Ser 396, AT8 and AT180 were significantly increased when Aβ₄₂ was expressed with -Dox (Figure 1B, N=4) compared to +Dox. p-Tau was also increased with Aβ₄₂ +Dox compared to LacZ +Dox. Parkin expression significantly reduced p-Tau levels (Figure 1B, N=4) when Aβ₄₂ was expressed with Dox, but Abl overexpression (-Dox) blocked Parkin’s effects on p-Tau levels. Western blot analysis

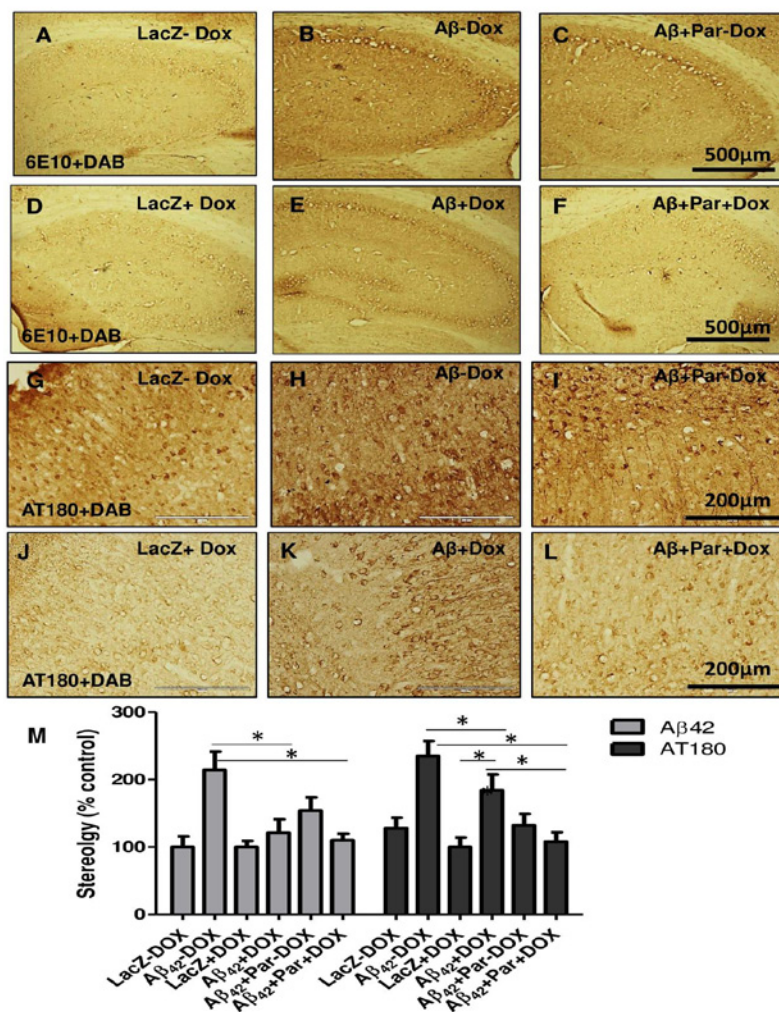


Figure 2: Abl activation exacerbates plaques and p-Tau accumulation. Immunostaining of 20µM thick sections with 6E10 antibody counterstained with DAB shows Aβ42 expression in the hippocampus of AblPP/tTA mice injected with (A). LacZ-Dox, (B). Aβ42-Dox, (C). Aβ42+Parkin-Dox, (D). LacZ+Dox, (E). Aβ42+Dox and (F). Aβ42+Parkin+Dox. Immunostaining with Tau antibody AT8+DAB shows p-Tau level in the hippocampus injected with (G). LacZ-Dox, (H). Aβ42-Dox, (I). Aβ42+Parkin-Dox, (J). LacZ+Dox, (K). Aβ42+Dox and (L). Aβ42+Parkin+Dox. Immunohistochemistry with AT180+DAB shows p-Tau in the cortex of mice injected with (M). LacZ-Dox, (N). Aβ42-Dox, (O). Aβ42+Parkin-Dox, (P). LacZ+Dox, (Q). Aβ42+Dox and (R). Aβ42+Parkin+Dox. (M). Histograms represent stereology. Graphs are mean±SEM, ANOVA with Neumann Keuls multiple comparison. N=4, asterisks are statistically significant compare to same treatment ±Dox or as indicated on graph. *indicates p<0.05.

supports ELISA measurement as shown in Suppl Figure 1.

The level of endogenous α-Synuclein was also significantly increased (Figure 1C, N=4) when Aβ42 was expressed with -Dox, but Parkin expression only reduced α-Synuclein with +Dox, further indicating Abl effects on protein accumulation. Western blot analysis (Figure 1D, p<0.05) shows increased levels of endogenous monomeric (34% via densitometry) and 60kDa higher molecular weight α-Synuclein (28%) with Aβ42-Dox compared to +Dox. LacZ-Dox (Figure 1D, lane 4) also increases the level (18%) of high molecular weight α-Synuclein. Lentiviral expression of human 4R Tau results in significant increases in Ser 396, AT8 and AT180 (Figure 1E, N=4, p<0.05) in -Dox compared to +Dox and LacZ control. Parkin expression significantly reduced p-Tau (Figure 1E, N=4, p<0.05)

back to LacZ levels when Tau was expressed with +Dox, but -Dox prevented Parkin effects on p-Tau reduction. Levels of α-Synuclein were also significantly increased (Figure 1F and Figure 1G, N=4) when Tau was expressed with -Dox. Parkin expression reduced α-Synuclein in the presence of +Dox, but Parkin was ineffective at reducing α-Synuclein when Abl was induced with -Dox.

Abl activation exacerbates plaques and p-tau accumulation

Lentiviral Aβ42 expression results in robust 6E10 staining in hippocampus of AblPP/tTA mice treated with either -Dox (Figure 2B) or +Dox (Figure 2E) compared to LacZ lentiviral control (Figure 2A and Figure 2D). Stereological counting shows 42% (N=4, p<0.05) reduction in 6E10-positive cells with +Dox (Figure 2E and Figure 2M, p<0.05) compared to -Dox (Figure 2B and Figure 2M).

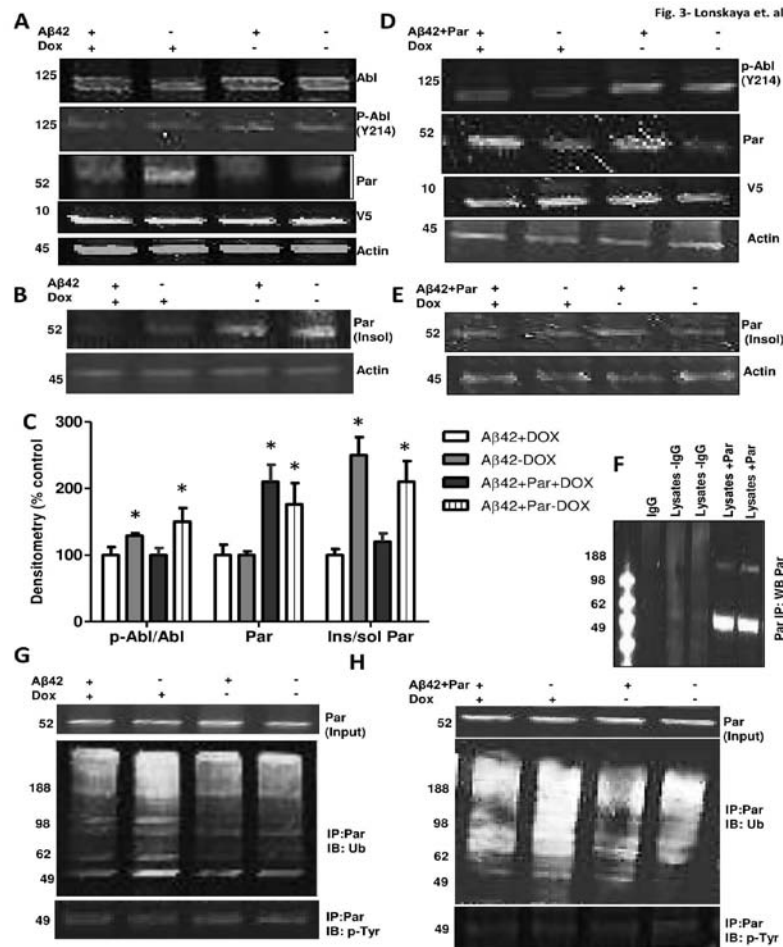


Figure 3: Abl activation reduces Parkin ubiquitination and solubility. Western blots on soluble brain lysates extracted in 1xSTEN buffer show (A). Total (1st blot) and phosphorylated Abl (Y412) in Aβ42 injected AbPP/tTA mice and Parkin level (3rd blot) relative to V5 and actin 6 weeks after Dox withdrawal and (B). insoluble Parkin extracted in 4M urea relative to actin (C). Histograms represent densitometry analysis of p-Abl/Abl and Parkin levels (D). Phosphorylated Abl in Aβ42+Parkin injected AbPP/tTA mice and Parkin level (2nd blot) relative to V5 and actin and (E). insoluble Parkin extracted in 4M urea relative to actin (F). Control experiments showing Parkin antibody specificity in the absence of IgG for Parkin (G and H). Immunoprecipitated Parkin (1st blot) probed with anti-ubiquitin (2nd blot) and anti-tyrosine (3rd blot) antibodies.

N=4, P<0.05. Bars are mean±SEM, ANOVA with Neumann Keuls multiple comparison. N=4, asterisks are statistically significant compare to same treatment ±Dox or as indicated on graph. *is p<0.05.

expression with Aβ42 reduced 6E10 staining to control levels with +Dox (Figure 2F and Figure 2M, p<0.05) whereas 6E10 staining was only reduced by 28% (N=4, p<0.05) with -Dox (Figure 2C and Figure 2M). Significant changes (28%, p<0.05, N=4) in the cortex were detected in p-Tau (AT180) when LacZ was expressed with -Dox (Figure 2G and Figure 2M) compared to +Dox (Figure 2J and Figure 2M). p-Tau was increased (84% by stereology) with Aβ42 expression -Dox (Figure H, Figure N and Figure M, p<0.05, N=4) compared to LacZ-Dox (Figure 2G and Figure 2M) and Parkin co-expression reduced (52%) p-Tau (Figure 2I and Figure 2M). p-Tau was also increased (80% by stereology) with Aβ42+Dox (Figure 2K and Figure 2M, p<0.05, N=4) compared to LacZ+Dox (Figure 2J and Figure 2M) and Parkin co-expression (Figure 2L and Figure 2M) reversed p-Tau to LacZ+Dox (Figure 2J and Figure 2M). Supplementary Figure 2 shows that Abl activation (-Dox) also worsens p-Tau accumulation.

Abl activation reduces parkin ubiquitination and solubility

To verify Abl activation, total and phosphorylated Abl (p-Abl) at tyrosine 412 (Y412) were analyzed with WB following Dox withdrawal for 6 weeks. Dox withdrawal (-Dox) increased Abl phosphorylation (Y412) compared to +Dox relative to total Abl (Figure 3A and Figure 3C, 29%, N=4, p<0.05), actin and V5 levels (32%). This was seen in the presence or absence of Aβ42 expression, but Aβ42 alone also increased total Abl levels (Figure 3A, 1st blot) with +Dox without any effects on p-Abl. Soluble endogenous Parkin level was decreased in -Dox alone or with Aβ42±Dox (Figure 3A and Figure 3C, p<0.05) relative to actin or V5 levels. Insoluble Parkin (extracted in 4M urea) was significantly higher relative to soluble Parkin in -Dox (Figure 3B and Figure 3C, N=4, p<0.05) compared to +Dox relative to actin, indicating that Abl activation reduces Parkin stability or decreases its solubility. A similar increase in active phosphorylated Abl (p-Abl Y214) was observed with -Dox when Parkin was co-expressed with Aβ42 (Figure 3D and

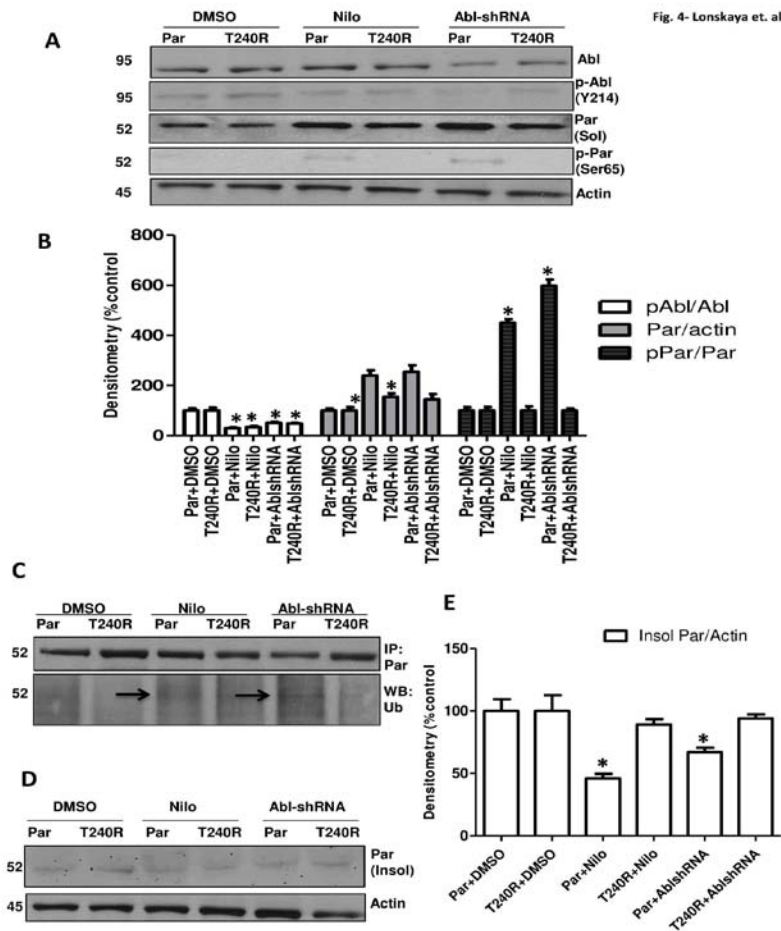


Figure 4: Abl inhibition increases Parkin ubiquitination and solubility. Western blots on soluble lysates (extracted in 1xSTEN buffer) of human M17 neuroblastoma cells over-expressing wild type Parkin or the non-catalytic T240R mutant and treated with Abl inhibitor Nilotinib or transfected with human Abl shRNA showing (A). Total (1st blot) Abl and phosphorylated (2nd blot) Abl (Y412), total Parkin (3rd blot) and Parkin phosphorylated at serine 65 (4th blot) relative to actin (B). Densitometry analysis (C). Immunoprecipitated soluble Parkin (1st blot) probed with anti-ubiquitin antibodies (2nd blot) (D). Western blots on insoluble lysates (extracted in 4M urea) showing Parkin levels relative to actin (E). Densitometry insoluble Parkin relative to actin. Mean±SEM, ANOVA with Neumann Keuls multiple comparison. N=6, asterisks are statistically significant compare to DMSO. *p*<0.05.

Figure 3C, *p*<0.05), and insoluble Parkin was also increased (Figure 3B, Figure 3E and Figure 3C, *p*<0.05) relative to soluble Parkin in -Dox. To determine possible Parkin modifications that alter its stability, Parkin was immunoprecipitated (Figure 3F is a control blot showing immunoprecipitated parkin detection in the presence and absence of Parkin antibody) and probed with anti-ubiquitin antibodies (Figure 3G and Figure 3H), which showed decreased levels of ubiquitinated protein smears (Figure 3G and Figure 3F) when Abl was activated (-Dox) compared to +Dox without Aβ42 expression in the presence or absence of Parkin over-expression. Total anti-tyrosine antibodies did not show any difference in Parkin phosphorylation at tyrosine ±Dox (Figure 3G and Figure 3F). Abl activation when Tau was expressed also significantly reduced soluble Parkin and increased insoluble Parkin shown in Suppl Figure 3.

Abl inhibition increases parkin ubiquitination and solubility

To verify whether Abl activity affects Parkin, human neuroblastoma cells over-expressing either human wild type Parkin or the catalytically inactive T240R Parkin mutant were treated

with Abl inhibitor Nilotinib or transfected with Abl shRNA for 24 hours as we previously described [24,25,31]. Nilotinib significantly (*P*<0.05, N=6) reduced p-Abl (Y214) levels (Figure 4A and Figure 4B, *p*<0.05) and Abl knockdown via shRNA significantly reduced total Abl (N=6, 56%) and p-Abl levels (Figure 4A and Figure 4B). Nilotinib and Abl shRNA significantly increased (*P*<0.05, N=6) total Parkin levels (Figure 4A and Figure 4B, *p*<0.05). The slight increase in Parkin in T240R lanes (Figure 4A, 3rd blot) is perhaps due to the effects of Abl inhibition on endogenous Parkin. Interestingly, Parkin phosphorylation on serine 65 was only detected when wild type Parkin but not mutant T240R was over-expressed (Figure 4A and Figure 4B). Parkin immunoprecipitation (Figure 4C, top blot) also showed that wild type Parkin but not T240R mutant is ubiquitinated (Figure 4C, 2nd blot, N=6). Insoluble wild type Parkin was significantly reduced (Figure 4D and Figure 4E, *P*<0.05, N=6) with Nilotinib and Abl knockdown (via shRNA), suggesting that Abl inhibition increases Parkin ubiquitination and serine 65 phosphorylation.

Abl activation reduces parkin ubiquitination

Parkin was immunoprecipitated from brain lysates and its

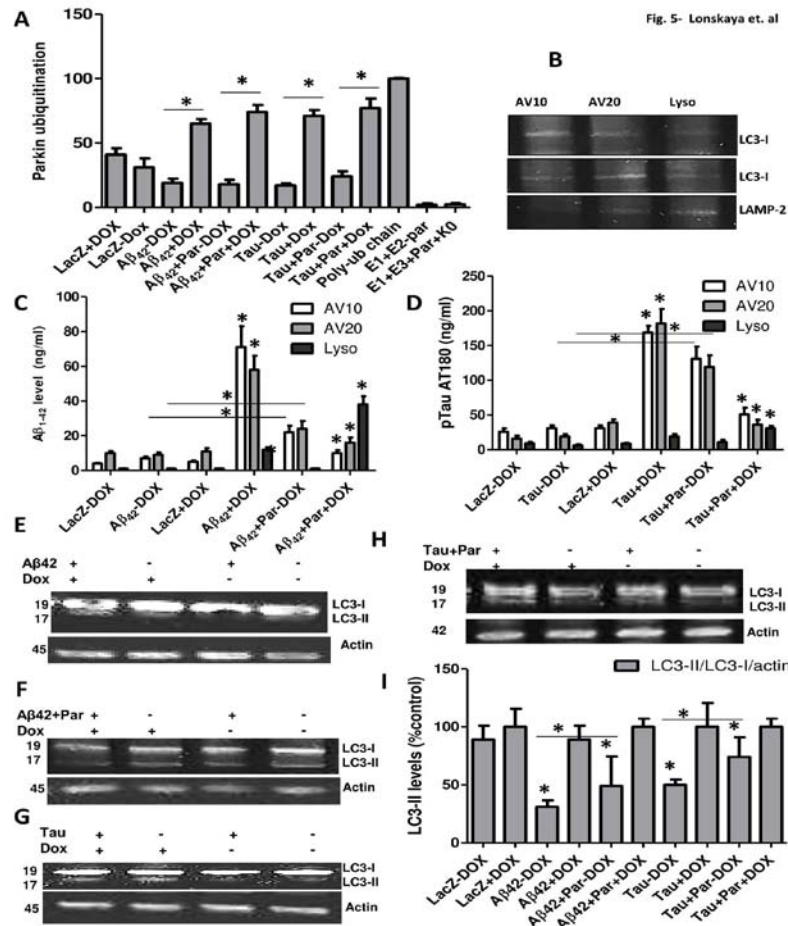


Figure 5: Abl activation reduces Parkin ubiquitination and impairs autophagy. (A). Parkin was immunoprecipitated from total brain lysates and ubiquitination was measured with E3LITE using poly-ubiquitin chains and Lysine-null ubiquitin (K0) as controls (B). Autophagic Vacuoles (AVs) were isolated and probed with Western blot with LC3 as pre-lysosomal (AV10 and AV20) marker and LAMP-2a as lysosomal marker (C). Human Aβ42 concentration in autophagic vacuoles in Aβ42 expressing brains with and without Parkin and (D). Tau concentration in autophagic vacuoles in Tau expressing brains with and without Parkin after 6 weeks Dox withdrawal. Western blots analysis showing LC3-I conversion to LC3-II relative to actin in (E). Aβ42 and (F). Aβ42+Parkin expressing brains. LC3-I conversion to LC3-II relative to actin in (G). Tau and (H). Tau+Parkin expressing brains (I). histograms represent LC3-II levels expressed as % control. Bars are mean±SEM, ANOVA with Neumann Keuls multiple comparison. N=4, asterisks are statistically significant compare to same treatment ±Dox or as indicated on graph. * indicates $p < 0.05$.

ubiquitination level was measured as previously described [24,25] using poly-ubiquitin chains and Lysine-null ubiquitin (K0) as controls (Figure 5A). Poly-ubiquitinated Parkin was significantly increased (Figure 4A, N=4, $P < 0.05$) when Aβ42 or Tau were expressed in the presence or absence of Parkin in +Dox compared to -Dox conditions, which were slightly lower than LacZ, indicating that Abl activation reduces Parkin ubiquitination.

Abl activation impairs autophagy and parkin enhances autophagic clearance

We previously demonstrated the effects of Abl inhibition on Parkin function and autophagic flux either via Abl shRNA knockdown or through pharmacological inhibition with Nilotinib in B35 rat neuroblastoma cells [25]. To evaluate autophagic flux in vivo, Autophagic Vacuoles (AVs) were isolated using Light Chain protein (LC)-3 to identify pre-lysosomal (AV10 and AV20) vacuoles (Figure 5B) and Lysosome Associated Membrane Protein (LAMP)-2 as a lysosomal marker as previously described [24,25]. Human

Aβ42 ELISA shows a significant increase in Aβ42 in pre-lysosomal vacuoles and lysosome +DOX compared to -Dox (Figure 5C, N=4, $p < 0.05$) when Aβ42 was expressed alone. No Aβ42 was detected -Dox suggesting that Abl activation impairs autophagic activity, but Parkin co-expression with Aβ42 significantly increased Aβ42 in pre-lysosomal vacuoles -DOX (Figure 5C, $P < 0.05$). Interestingly, Parkin co-expression with Aβ42+Dox significantly reduced Aβ42 in pre-lysosomal fractions and increased it in the lysosome (Figure 5C, N=4, $P < 0.05$), indicating that Parkin facilitates lysosomal Aβ42 clearance. Tau ELISA (AT180) shows a significant increase in p-Tau in pre-lysosomal vacuoles +DOX compared to -Dox (Figure 5D, N=4, $p < 0.05$) when Tau was expressed alone. No p-Tau was detected in Tau-Dox but Parkin co-expression with Tau significantly increased p-Tau in pre-lysosomal vacuoles -DOX (Figure 5D, $P < 0.05$). Similarly, Parkin co-expression with Tau+Dox significantly reduced p-Tau in pre-lysosomal vacuoles and increased in the lysosome (Figure 5D, N=4, $P < 0.05$). The conversion of LC3-I to LC3-II as a marker of autophagic activity was not different in LacZ

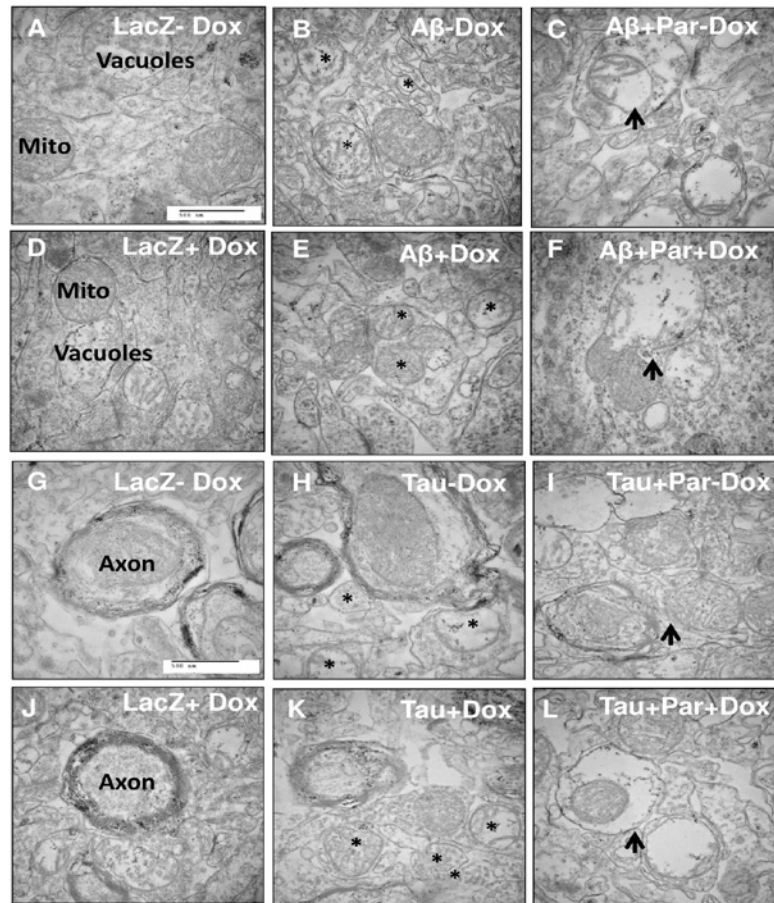


Figure 6: Parkin expression increases autophagic clearance. Electron micrographs of AblPP/tTA brains injected with (A). LacZ-Dox, (B). A β 42-Dox, asterisks indicate accumulation of cytosolic vesicles (C). A β 42+Parkin-Dox, arrows indicate large vacuole formation (D). LacZ+Dox, (E). A β 42+Dox, asterisks indicate accumulation of cytosolic vesicles (F). A β 42+Parkin+Dox, arrows indicate large vacuole formation (G). LacZ-Dox, (H). Tau-Dox, asterisks indicate accumulation of cytosolic vesicles (I). Tau+Parkin-Dox, arrows indicate large vacuole formation (L). LacZ+Dox, (M). Tau+Dox, asterisks indicate accumulation of cytosolic vesicles (L). Tau+Parkin+Dox, arrows indicate large vacuole formation. N=4.

-Dox compared to +Dox (Figure 5E, Figure 5F, Figure 5G, Figure 5H and Figure 5I). Expression of A β 42 (Figure 5E and Figure 5I) or Tau (Figure 4G and Figure 4I) result in significantly lower LC3-II with -Dox compared to +Dox relative to LC3-I. Parkin expression with A β 42 (Figure 5F and Figure 5I) and Tau (Figure 5H and Figure 5I) result in significantly lower levels of LC3-II with -Dox compared to +Dox and Parkin expression with A β 42 or Tau increases autophagic flux (Figure 5I, N=4, $p < 0.05$).

Parkin expression increases autophagic clearance

Electron micrographs do not show any noticeable differences between LacZ-Dox (Figure 6A and Figure 6G) and LacZ+Dox (Figure 6D and Figure 6J). Electron micrographs are representative of N=4 animals in each treatment arm of this study. A β 42 or Tau expression is associated with accumulation of cytosolic vesicles (asterisks) with -Dox (Figure 6C and Figure 6H, N=4) and +Dox (Figure 6E and Figure 6K, N=4), but Parkin expression results in formation of larger vacuoles (Figure 6C, Figure 6F, Figure 6I and Figure 6L. Arrows that may be indicative of enhanced autophagic clearance. Supplementary Figure 4 shows that Abl activation (-Dox) increases cell death.

Discussion

The current data show that Abl activity reduces Parkin function

and arrests autophagic clearance of p-Tau and A β 42 in the brain of AblPP/tTA mice. Previous reports suggest that Abl activation regulates Parkin function via tyrosine phosphorylation [2,4]. Our data show that Abl activation regulates Parkin ubiquitination and activity. However, it is unclear whether Abl is acting directly to phosphorylate Parkin, or indirectly to either phosphorylate ubiquitin or to activate another Ser/Thr kinase that phosphorylates Parkin. Our data are consistent with the effects of Parkin phosphorylation (serine 65) and ubiquitination on its activity (reviewed in [32]). Parkin activation via ubiquitination is congruent with its structure that contains 9 potential ubiquitination sites [33], suggesting that ubiquitination activates Parkin to transfer ubiquitin onto its substrates. Parkin has a complex structure and it is usually auto-inhibited [33-36] but it may be activated in response to cellular stress. Recent structural analysis of Parkin in auto-inhibited state demonstrates Parkin activation via ubiquitination [35,36]. In response to mitochondrial depolarization, PTEN-Induced Putative Kinase-1 (PINK1) phosphorylates Serine 65 on Parkin [37] to activate it. PINK1 also modifies ubiquitin at Serine 65, which is homologous to the site phosphorylated in Parkin [38-41]. Ubiquitin phosphorylation by PINK1 promotes Parkin phosphorylation at Serine residues and activation via self-ubiquitination [40,42]. We previously demonstrated that Parkin is

auto-ubiquitinated, leading to ubiquitination of TAR DNA binding protein (TDP)-43 [43]. Parkin ubiquitination may enhance the E3 ubiquitin ligase activity and affect its stability [23,25,38,39,41]. The current results show that Parkin ubiquitination proceeds under conditions of normal Abl activity, but increased Abl activity reduces Parkin ubiquitination and solubility, suggesting that Abl reduces Parkin function via loss of protein stability. Parkin ubiquitination may stabilize a basal level of active Parkin. For example, the increased level of insoluble Parkin in post-mortem AD [19] and sporadic PD [17] brains suggests an imbalance between ubiquitinated and non-ubiquitinated Parkin levels. Decreased Parkin ubiquitination may lead to lack of proteasome recognition, perhaps increasing its inactive/insoluble levels. It is unclear whether de-ubiquitination reduces Parkin degradation, thus stabilizing its steady state levels and activity, or alternatively, contributes to inactivation. Recent work demonstrates that the Ubiquitin Specific Protease (USP)-8 directly de-ubiquitinates Parkin via selective removal of Lysine6-linked ubiquitin chains and decreases autophagic activity [44], consistent with the hypothesis that Parkin de-ubiquitination can abrogate its activity.

Evidence suggests that $A\beta$ and p-Tau accumulation in AD may be a result of reduced autophagic clearance [45-52], thus stimulation of autophagy is one mechanism to degrade $A\beta$ and p-Tau. We previously documented evidence that Abl activation is associated with p-Tau and $A\beta$ accumulation in several AD models [3,5-7,22,24,25,53,54] and human post-mortem AD brains [22,24,55]. Pharmacological Abl inhibition promotes autophagic degradation of $A\beta$ and p-Tau and improves cognition [22-25], while the current data show that Abl activation reduces Parkin function and blocks autophagic flux. Together these results point to Abl as a drug target to activate Parkin and facilitate autophagic clearance of amyloidogenic proteins.

The data demonstrate a role for Parkin activity beyond Parkin's established function in inherited PD. The ability of Parkin to regulate $A\beta$ and p-Tau levels and autophagic activities, and the modulation of Parkin's actions by Abl, also indicate a role for Parkin in AD pathology. Loss of Parkin solubility in AD suggests reduced activity that results in impairment of interaction with autophagy enzymes as previously demonstrated [21-25]. Abl inhibitors that penetrate the brain and increase Parkin ubiquitination and stability may promote autophagic protein degradation and reduce neurodegeneration. Therefore, Parkin dysfunction via mutations or protein instability may lead to neurodegeneration, but its activity constitutes a quality control sensor to counteract protein accumulation. Abl inhibition is therefore an alternative strategy to activate Parkin as a therapeutic target for neurodegenerative diseases, including AD.

References

- Wang JY. Regulation of cell death by the Abl tyrosine kinase. *Oncogene*. 2000; 19: 5643-5650.
- Imam SZ, Zhou Q, Yamamoto A, Valente AJ, Ali SF, Bains M, et al. Novel regulation of parkin function through c-Abl-mediated tyrosine phosphorylation: implications for Parkinson's disease. *J Neurosci*. 2011; 31: 157-163.
- Jing Z, Caltagarone J, Bowser R. Altered subcellular distribution of c-Abl in Alzheimer's disease. *J Alzheimers Dis*. 2009; 17: 409-422.
- Ko HS, Lee Y, Shin JH, Karuppagounder SS, Gadad BS, Koleske AJ, et al. Phosphorylation by the c-Abl protein tyrosine kinase inhibits parkin's ubiquitination and protective function. *Proc Natl Acad Sci USA*. 2010; 107: 16691-16696.
- Tremblay MA, Acker CM, Davies P. Tau phosphorylated at tyrosine 394 is found in Alzheimer's disease tangles and can be a product of the Abl-related kinase, Arg. *J Alzheimers Dis*. 2010; 19: 721-733.
- Derkinderen P, Scales TM, Hanger DP, Leung KY, Byers HL, Ward MA, et al. Tyrosine 394 is phosphorylated in Alzheimer's paired helical filament tau and in fetal tau with c-Abl as the candidate tyrosine kinase. *J Neurosci*. 2005; 25: 6584-6593.
- Schlatterer SD, Acker CM, Davies P. c-Abl in neurodegenerative disease. *J Mol Neurosci*. 2011; 45: 445-452.
- Cancino GI, Perez de Arce K, Castro PU, Toledo EM, von Bernhardi R, Alvarez AR. c-Abl tyrosine kinase modulates tau pathology and Cdk5 phosphorylation in AD transgenic mice. *Neurobiol Aging*. 2011; 32: 1249-1261.
- Cancino GI, Toledo EM, Leal NR, Hernandez DE, Yevenes LF, Inestrosa NC, et al. STI571 prevents apoptosis, tau phosphorylation and behavioural impairments induced by Alzheimer's beta-amyloid deposits. *Brain*. 2008; 131: 2425-2442.
- Alvarez AR, Sandoval PC, Leal NR, Castro PU, Kosik KS. Activation of the neuronal c-Abl tyrosine kinase by amyloid-beta-peptide and reactive oxygen species. *Neurobiol Dis*. 2004; 17: 326-336.
- Karuppagounder SS, Brahmachari S, Lee Y, Dawson VL, Dawson TM, Ko HS. The c-Abl inhibitor, nilotinib, protects dopaminergic neurons in a preclinical animal model of Parkinson's disease. *Sci Rep*. 2014; 4: 4874.
- Geisler S, Holmstrom KM, Skujat D, Fiesel FC, Rothfuss OC, Kahle PJ, et al. PINK1/Parkin-mediated mitophagy is dependent on VDAC1 and p62/SQSTM1. *Nat Cell Biol*. 2010; 12: 119-131.
- Narendra D, Tanaka A, Suen DF, Youle RJ. Parkin is recruited selectively to impaired mitochondria and promotes their autophagy. *J Cell Biol*. 2008; 183: 795-803.
- Park J, Kim Y, Chung J. Mitochondrial dysfunction and Parkinson's disease genes: insights from *Drosophila*. *Dis Model Mech*. 2009; 2: 336-340.
- Vives-Bauza C, Zhou C, Huang Y, Cui M, de Vries RL, Kim J, et al. PINK1-dependent recruitment of Parkin to mitochondria in mitophagy. *Proc Natl Acad Sci USA*. 2010; 107: 378-383.
- Kitada T, Asakawa S, Hattori N, Matsumine H, Yamamura Y, Minoshima S, et al. Mutations in the parkin gene cause autosomal recessive juvenile parkinsonism. *Nature*. 1998; 392: 605-608.
- Lonskaya I, Hebron ML, Algarzae NK, Desforges N, Moussa CE. Decreased parkin solubility is associated with impairment of autophagy in the nigrostriatum of sporadic Parkinson's disease. *Neuroscience*. 2013; 232: 90-105.
- Lonskaya I, Shekoyan AR, Hebron ML, Desforges N, Algarzae NK, Moussa CE. Diminished parkin solubility and co-localization with intraneuronal amyloid-beta are associated with autophagic defects in Alzheimer's disease. *J Alzheimers Dis*. 2013; 33: 231-247.
- Lonskaya I, Shekoyan AR, Hebron ML, Desforges N, Algarzae NK, Moussa CE. Diminished parkin solubility and co-localization with intraneuronal amyloid-beta are associated with autophagic defects in Alzheimer's disease. *J Alzheimers Dis*. 2013; 33: 231-247.
- Herman AM, Moussa CE. The ubiquitin ligase parkin modulates the execution of autophagy. *Autophagy*. 2011; 7: 919-921.
- Khandelwal PJ, Herman AM, Hoe HS, Rebeck GW, Moussa CE. Parkin mediates beclin-dependent autophagic clearance of defective mitochondria and ubiquitinated Abeta in AD models. *Hum Mol Genet*. 2011; 20: 2091-2102.
- Hebron ML, Lonskaya I, Moussa CE. Nilotinib reverses loss of dopamine neurons and improves motor behavior via autophagic degradation of alpha-synuclein in Parkinson's disease models. *Hum Mol Genet*. 2013; 22: 3315-3328.
- Lonskaya I, Desforges NM, Hebron ML, Moussa CE. Ubiquitination Increases Parkin Activity to Promote Autophagic alpha-Synuclein Clearance. *PLoS One*. 2013.

24. Lonskaya I, Hebron ML, Desforgues NM, Franjie A, Moussa CE. Tyrosine kinase inhibition increases functional parkin-Beclin-1 interaction and enhances amyloid clearance and cognitive performance. *EMBO Mol Med*. 2013; 5: 1247-1262.
25. Lonskaya I, Hebron ML, Desforgues NM, Schachter JB, Moussa CE. Nilotinib-induced autophagic changes increase endogenous parkin level and ubiquitination, leading to amyloid clearance. *J Mol Med(Berl)*. 2014; 92: 373-386.
26. Schlatterer SD, Tremblay MA, Acker CM, Davies P. Neuronal c-Abl overexpression leads to neuronal loss and neuroinflammation in the mouse forebrain. *J Alzheimers Dis*. 2011; 25: 119-133.
27. Burns MP, Zhang L, Rebeck GW, Querfurth HW, Moussa CE. Parkin promotes intracellular Abeta₁₋₄₂ clearance. *Hum Mol Genet*. 2009; 18: 3206-3216.
28. Khandelwal PJ, Dumanis SB, Feng LR, Maguire-Zeiss K, Rebeck G, Lashuel HA, et al. Parkinson-related parkin reduces alpha-Synuclein phosphorylation in a gene transfer model. *Mol Neurodegener*. 2010; 5: 47.
29. Khandelwal PJ, Dumanis SB, Herman AM, Rebeck GW, Moussa CE. Wild type and P301L mutant Tau promote neuro-inflammation and alpha-Synuclein accumulation in lentiviral gene delivery models. *Mol Cell Neurosci*. 2012; 49: 44-53.
30. Marzella L, Ahlberg J, Glaumann H. Isolation of autophagic vacuoles from rat liver: morphological and biochemical characterization. *J Cell Biol*. 1982; 93: 144-154.
31. Lonskaya I, Hebron M, Chen W, Schachter J, Moussa C. Tau deletion impairs intracellular beta-amyloid-42 clearance and leads to more extracellular plaque deposition in gene transfer models. *Mol Neurodegener*. 2014; 9: 46.
32. Moussa CE. Parkin Is Dispensable for Mitochondrial Function, but Its Ubiquitin Ligase Activity Is Critical for Macroautophagy and Neurotransmitters: Therapeutic Potential beyond Parkinson's Disease. *Neurodegener Dis*. 2015; 15: 259-270.
33. Riley BE, Loughheed JC, Callaway K, Velasquez M, Brecht E, Nguyen L, et al. Structure and function of Parkin E3 ubiquitin ligase reveals aspects of RING and HECT ligases. *Nat Commun*. 2013; 4: 1982.
34. Matsuda N, Sato S, Shiba K, Okatsu K, Saisho K, Gautier CA, et al. PINK1 stabilized by mitochondrial depolarization recruits Parkin to damaged mitochondria and activates latent Parkin for mitophagy. *J Cell Biol*. 2010; 189: 211-221.
35. Trempe JF, Sauve V, Grenier K, Seirafi M, Tang MY, Menade M, et al. Structure of parkin reveals mechanisms for ubiquitin ligase activation. *Science*. 2013; 340: 1451-1455.
36. Wauer T, Komander D. Structure of the human Parkin ligase domain in an autoinhibited state. *EMBO J*. 2013; 32: 2099-2112.
37. Kondapalli C, Kazlauskaitė A, Zhang N, Woodroof HI, Campbell DG, Gourlay R, et al. PINK1 is activated by mitochondrial membrane potential depolarization and stimulates Parkin E3 ligase activity by phosphorylating Serine 65. *Open Biol*. 2012; 2: 120080.
38. Kane LA, Lazarou M, Fogel AI, Li Y, Yamano K, Sarraf SA, et al. PINK1 phosphorylates ubiquitin to activate Parkin E3 ubiquitin ligase activity. *J Cell Biol*. 2014; 205: 143-153.
39. Kazlauskaitė A, Kondapalli C, Gourlay R, Campbell DG, Ritorto MS, Hofmann K, et al. Parkin is activated by PINK1-dependent phosphorylation of ubiquitin at Ser65. *Biochem J*. 2014; 460: 127-139.
40. Kazlauskaitė A, Muqit MM. PINK1 and Parkin - mitochondrial interplay between phosphorylation and ubiquitylation in Parkinson's disease. *FEBS J*. 2015; 282: 215-223.
41. Koyano F, Okatsu K, Kosako H, Tamura Y, Go E, Kimura M, et al. Ubiquitin is phosphorylated by PINK1 to activate parkin. *Nature*. 2014; 510: 162-166.
42. Caulfield TR, Fiesel FC, Moussaud-Lamodièrè EL, Dourado DF, Flores SC, Springer W. Phosphorylation by PINK1 releases the UBL domain and initializes the conformational opening of the E3 ubiquitin ligase Parkin. *PLoS Comput Biol*. 2014.
43. Hebron ML, Lonskaya I, Sharpe K, Weerasinghe PP, Algarzàe NK, Shekoyan AR, et al. Parkin ubiquitinates Tar-DNA binding protein-43 (TDP-43) and promotes its cytosolic accumulation via interaction with histone deacetylase 6 (HDAC6). *J Biol Chem*. 2013; 288: 4103-4115.
44. Durcan TM, Tang MY, Perusse JR, Dashti EA, Aguilera MA, McLelland GL, et al. USP8 regulates mitophagy by removing K6-linked ubiquitin conjugates from parkin. *EMBO J*. 2014; 33: 2473-2491.
45. Boland B, Kumar A, Lee S, Platt FM, Wegiel J, Yu WH, et al. Autophagy induction and autophagosome clearance in neurons: relationship to autophagic pathology in Alzheimer's disease. *J Neurosci*. 2008; 28: 6926-6937.
46. Kegel KB, Kim M, Sapp E, McIntyre C, Castano JG, Aronin N, et al. Huntingtin expression stimulates endosomal-lysosomal activity, endosome tubulation, and autophagy. *J Neurosci*. 2000; 20: 7268-7278.
47. Nixon RA. The role of autophagy in neurodegenerative disease. *Nature medicine*. 2013; 19: 983-997.
48. Nixon RA, Wegiel J, Kumar A, Yu WH, Peterhoff C, Cataldo A, et al. Extensive involvement of autophagy in Alzheimer disease: an immunoelectron microscopy study. *J Neuropathol Exp Neurol*. 2005; 64: 113-122.
49. Ravikumar B, Duden R, Rubinsztein DC. Aggregate-prone proteins with polyglutamine and polyalanine expansions are degraded by autophagy. *Hum Mol Genet*. 2002; 11: 1107-1117.
50. Sabatini DM. mTOR and cancer: insights into a complex relationship. *Nat Rev Cancer*. 2006; 6: 729-734.
51. Stefanis L, Larsen KE, Rideout HJ, Sulzer D, Greene LA. Expression of A53T mutant but not wild-type alpha-synuclein in PC12 cells induces alterations of the ubiquitin-dependent degradation system, loss of dopamine release, and autophagic cell death. *J Neurosci*. 2001; 21: 9549-9560.
52. Webb JL, Ravikumar B, Atkins J, Skepper JN, Rubinsztein DC. Alpha-Synuclein is degraded by both autophagy and the proteasome. *J Biol Chem*. 2003; 278: 25009-25013.
53. Hebron ML, Lonskaya I, Moussa CE. Tyrosine kinase inhibition facilitates autophagic SNCA/alpha-synuclein clearance. *Autophagy*. 2013; 9: 1249-1250.
54. Mahul-Mellier AL, Fauvet B, Gysbers A, Dikiy I, Oueslati A, Georgeon S, et al. c-Abl phosphorylates alpha-synuclein and regulates its degradation: implication for alpha-synuclein clearance and contribution to the pathogenesis of Parkinson's disease. *Hum Mol Genet*. 2014; 23: 2858-2879.
55. Salomoni P, Calabretta B. Targeted therapies and autophagy: new insights from chronic myeloid leukemia. *Autophagy*. 2009; 5: 1050-1051.